THE "CHUNNEL" FIRE. I: CHEMOPLASTIC SOFTENING IN RAPIDLY HEATED CONCRETE

By Franz-Josef Ulm,[1] Olivier Coussy,[2] and Zdeněk P. Bažant[3]

ABSTRACT: This paper and its companion paper present the main results of an assessment of the fire in the Channel Tunnel (the "Chunnel"), which destroyed a part of the concrete tunnel rings by thermal spalling. The study seeks (1) to evaluate the effect of thermal damage (loss of elastic stiffness) and thermal decohesion (loss of material strength) upon the stress state and cracking at a structural level; and (2) to check whether restrained thermal dilatation can explain the thermal spalling observed during the fire. In the present paper, a macroscopic material model for rapidly heated concrete is developed. It accounts explicitly for the dehydration of concrete and its cross-effects with deformation (chemomechanical couplings) and temperature (chemothermal couplings). The thermal decohesion is considered as chemoplastic softening within the theoretical framework of chemoplasticity. Furthermore, kinetics of dehydration, dimensional analysis, and thermodynamic equilibrium considerations show that a unique thermal dehydration function exists that relates the hydration degree to the temperature rise, provided that the characteristic time of dehydration is much inferior to the characteristic time of structural heat conduction. The experimental determination of the thermal dehydration function from in-situ measurements of the elastic modulus versus furnace temperature rise is shown from experimental data available from the chunnel concrete. Finally, by way of an example, the proposed constitutive model for rapidly heated concrete is combined with the three-parameter William-Warnke criterion extended to isotropic chemoplastic softening.

INTRODUCTION

On November 18, 1996, a fire of 10 h duration with temperatures up to 700°C occurred in the Channel Tunnel (the "Chunnel"), the 35 km railroad transport tunnel connecting England and France. The fire destroyed parts of the concrete tunnel rings by thermal spalling over a length of a few hundred meters. Beside logistic questions concerning security and economic losses (a loss of $1.5 million per day over the six-month closure for repairs has been reported), the Chunnel fire revealed the lack of understanding of the underlying mechanisms that (1) govern the material behavior of concrete at high temperature (on the material level); and (2) lead to spalling of concrete members exposed to high temperatures (on the structural level). As far as the phenomena are concerned, both the material and structural behaviors are well described in the literature [for state-of-the-art reviews, see Schneider (1982), Bažant and Kaplan (1996), Phan (1997), and Phan et al. (1997)].

- On the material level, high temperatures lead to an irreversible loss of elastic stiffness (thermal damage) and of material strength (thermal decohesion) of concrete. On the macroscale of engineering material description (the typical scale of laboratory test specimens), thermal damage and thermal decohesion are generally described by an apparent temperature dependence of the material properties of concrete, as shown in Figs. 1(a and b) for the elastic modulus $E = E(T)$, and the compressive strength $f_c = f_c(T)$. Some of this thermal damage and thermal decohesion may result from the difference in thermal dilatation coefficient between the aggregates and the cement paste, in particular in concretes with silicious aggregates. In turn, this is not the case of concretes with calcareous aggregates such as the one employed for the Chunnel rings, for which the thermal dilatation coefficients of the aggregates and the cement paste (almost) coincide. Hence, another phenom-

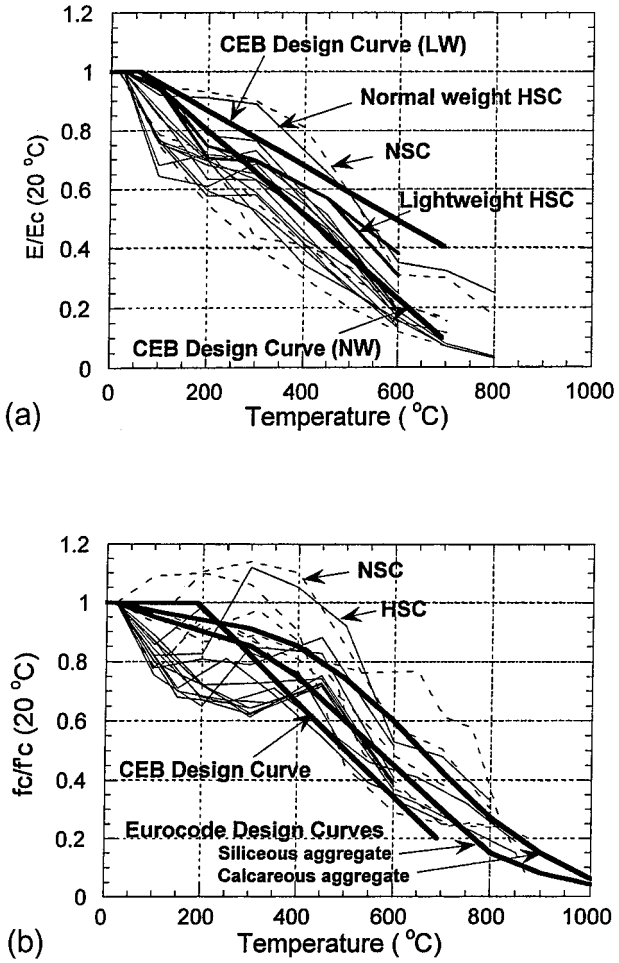

FIG. 1. (a) Thermal Damage (Thermal Loss of Elastic Stiffness), $E = E(T)$; (b) Thermal Decohesion (Thermal Strength Loss), $f_c = h_c(T)$ [from Compilation of Test Data by Phan (1997)]

[1]Res. Engr., Laboratoire Central des Ponts et Chaussées, Div. Bétons & Ciments pour Ouvrages d'Art, 58, Bd. Lefebvre, 75732 Paris Cedex 15, France; presently, Massachusetts Institute of Technology, Cambridge, MA 02139. E-mail: ulm@mit.edu

[2]Res. Dir., Laboratoire Central des Ponts et Chaussées, Service Modélisation pour l'Ingénieur, 58, Bd. Lefebvre, 75732 Paris Cedex 15, France. E-mail: coussy@lcpc.fr

[3]Walter P. Murphy Prof. of Civ. Engrg. and Mat. Sci., Northwestern Univ., Evanston, IL 60208. E-mail: z-bazant@nwu.edu

Note. Associate Editor: Gilles Pijaudier-Cabot. Discussion open until August 1, 1999. Separate discussions should be submitted for the individual papers in this symposium. To extend the closing date one month, a written request must be filed with the ASCE Manager of Journals. The manuscript for this paper was submitted for review and possible publication on October 29, 1997. This paper is part of the ***Journal of Engineering Mechanics***, Vol. 125, No. 3, March, 1999. ©ASCE, ISSN 0733-9399/99/0003-0272–0282/$8.00 + $.50 per page. Paper No. 16923.

enon must be involved. From microstructural analysis of fire-damaged concrete it has been found that both thermal damage and thermal decohesion result rather from the dehydration of concrete on the microlevel [e.g., Lin et al. (1996)].
- On the structural level, the behavior of concrete members exposed to a large temperature rise is characterized by spalling, i.e., by a brittle failure with most fracture planes parallel to the heated surface. The risk of explosive thermal spalling has been found to be much more important for structural members made of high performance concretes, and seems to increase with the specimen size. The first can be explained by the higher brittleness of high performance concretes (material property) [e.g., Bažant (1997)], while the second seems to be related to the length scales of heat and moisture transport through the structure, as well as the capacity of larger structures to store more energy (and their higher brittleness number).

While thermal spalling is frequently observed on concrete members exposed to rapid heating, little agreement exists on its physical origin. One may distinguish two main explanations:

- Spalling due to pressure buildup (Anderberg 1997). The hypothesis is based on the low permeability of concrete. Pressures are generated by the temperature at the front of heating. The drained conditions at the heated surface and the low permeability of concrete lead to strong pressure gradients close to the surface, in the form of the so-called moisture clog (Harmathy 1965), as sketched in Fig. 2(a). The pore pressure is considered to drive progressive brittle failure, i.e., spalling—the more the lower the permeability of the concrete. This explanation seems consistent with the experimental observation that predried specimens are less prone to thermal spalling. Anyway, since spalling did occur in the Chunnel, predrying (in the 10 year old tunnel rings) seems not to have been sufficient to prevent it. Furthermore, it is worth noting that the order of magnitude of these pressures, experimentally determined or theoretically predicted, has never exceeded 1 MPa for normal strength concrete and 2 to 3 MPa for high performance concrete (Bažant and Thongutai 1978, 1979; Kontani 1994; Ahmed and Hurst 1995; Noumowé 1995; Consolazio et al. 1997).
- Spalling due to restrained thermal dilatation (Bažant 1997). The hypothesis considers that the spalling results from restrained thermal dilatation close to the heated surface, which leads to compressive stresses parallel to the heated surface. These compressive stresses are released by brittle fracture of concrete, i.e., spalling. The pore pressure can play only a secondary role as far as the growth of a larger crack is concerned, because, due to the volume expansion of a growing crack and the slowness of release of additional water into the crack, the pressure in the crack must rapidly decay after the crack begins to open. The pressure may affect the bifurcation and the onset of instability in the form of explosive thermal spalling [Fig. 2(b)]. This explanation seems consistent with the order of magnitude of pore pressures.

This paper and its companion paper (Ulm et al. 1999) present the main results of a study of the Chunnel fire contracted to Laboratoire Central des Ponts et Chaussées (LCPC), Paris. This study seeks (1) to evaluate the effect of thermal damage and thermal decohesion upon the stress state and cracking on the structural level; and (2) to check whether restrained thermal dilatation can explain the thermal spalling observed during the fire. The macroscopic modeling of the dehydration and its cross-effects with elastic deformation and irreversible changes in the solid skeleton is the purpose of this paper. The constitutive model will be developed in the framework of chemoplasticity (Coussy and Ulm 1996). It can be considered as an inverse case of the modeling of thermo-chemomechanical couplings in early-age concrete (Ulm and Coussy 1995, 1996) with chemoplastic softening due to dehydration. The results obtained with this model in finite-element analysis of the Chunnel fire are shown in the companion paper (Ulm et al. 1999).

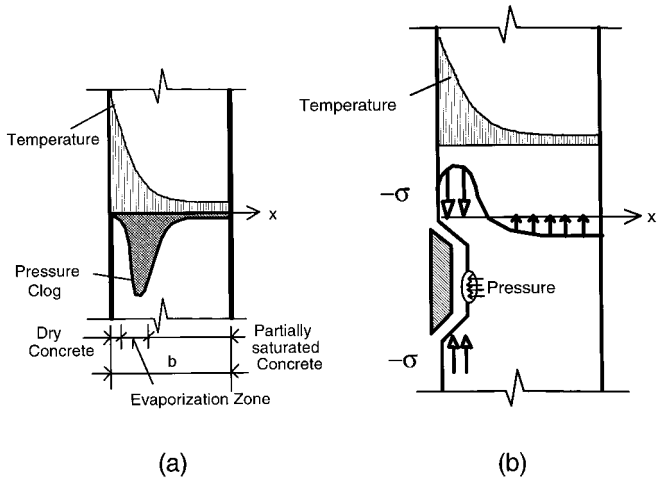

FIG. 2. Spalling Hypothesis: (a) Spalling Due to Pore Pressure Buildup according to Anderberg (1997); (b) Spalling as Brittle Fracture Due to Restrained Thermal Dilatation According to Bažant (1997)

CONSTITUTIVE MODEL

Consider concrete as a porous medium composed of a skeleton and some fluid phases filling the capillary pore space (i.e., water, vapor, and dry air). The observable strain is that of the solid skeleton, denoted as $\boldsymbol{\varepsilon}$. The cracking is considered here within the standard continuum approach of elastoplasticity by means of certain plastic variables, i.e., the plastic (or permanent) strain tensor, $\boldsymbol{\varepsilon}^p$, and the plastic hardening/softening variable χ, which both model the irreversible changes in the skeleton associated with microcracking. Furthermore, m_{sk} is denoted as the hydrate mass per unit of volume of concrete, which equals, with opposite sign, the dehydration mass expelled in liquid form from the micropores of cement gel into the capillary pore space. For the sake of simplicity, the elementary system is considered as closed (sealed) with respect to the fluid phases filling the macropore space. Obviously, this hypothesis, as well as the choice of plastic variables to represent cracking, is merely the first approach to the complex phenomena occurring under fire conditions in concrete. It must be seen in the perspective of the overall scope of this study, i.e., the evaluation of the risk of spalling due to restrained thermal dilatation in rapidly heated concrete. The brittle fracture analysis is beyond the scope of this study.

To formulate the couplings between dehydration, temperature, and deformation, the framework of chemically reactive porous continua is applied (Coussy 1995). To this end, consider the energy dissipation of the closed reactive porous material, which reads

$$\varphi = \boldsymbol{\sigma}:\dot{\boldsymbol{\varepsilon}} - S\dot{T} - \dot{\Psi} \geq 0 \tag{1}$$

where a dot denotes the time derivative; $\boldsymbol{\sigma}$ = macroscopic stress tensor; S = entropy; and Ψ = free (Helmholtz) energy per unit volume. The free energy Ψ is a function of the state

variables, which describe the energy state of the elementary system. These are the (absolute) temperature T and strain $\boldsymbol{\varepsilon}$ as the external state variables, and the plastic variables $\boldsymbol{\varepsilon}^p$ and χ as the internal state variables. Hydrate mass m_{sk} also is part of the set of internal state variables (i.e., variables not controlled from the exterior). The free energy Ψ is assumed in the form

$$\Psi = \Psi(T, \boldsymbol{\varepsilon}, \boldsymbol{\varepsilon}^p, \chi, m_{sk}) = \psi(T, \boldsymbol{\varepsilon} - \boldsymbol{\varepsilon}^p, m_{sk}) + U(\chi, m_{sk}) \quad (2)$$

where ψ = reduced potential; and U = frozen energy related to chemoplastic hardening/softening. Using (2) in (1) yields

$$\varphi = \varphi_1 + \varphi_c \geq 0 \quad (3a)$$

$$\varphi_1 = \boldsymbol{\sigma}:\dot{\boldsymbol{\varepsilon}}^p + \zeta\dot{\chi} \geq 0; \quad \varphi_c = A_m\dot{m}_{sk} \geq 0 \quad (3b,c)$$

with

$$\boldsymbol{\sigma} = \frac{\partial\psi}{\partial\boldsymbol{\varepsilon}} = -\frac{\partial\psi}{\partial\boldsymbol{\varepsilon}^p}; \quad S = -\frac{\partial\Psi}{\partial T} \quad (4a,b)$$

$$\zeta = -\frac{\partial U}{\partial\chi}; \quad A_m = -\frac{\partial(\psi + U)}{\partial m_{sk}} \quad (4c,d)$$

where φ_1 = energy dissipation rate associated with plastic deformations (including plastic hardening/softening); and φ_c = energy dissipation rate associated with the dehydration process. In (3) and (4), the stress tensor $\boldsymbol{\sigma}$ has been classically designated as the driving force of plastic strains, and the hardening force ζ as the force associated with plastic hardening or softening. In the same manner, A_m is the driving force of the dehydration process, and is called the affinity. The energy approach allows one to derive the chemothermal and chemomechanical cross-effects from the Maxwell symmetries of potentials ψ and U. In particular, for the dehydration process at hand, the couplings are presented by

$$\frac{\partial S}{\partial m_{sk}} = \frac{\partial A_m}{\partial T} = -\frac{\partial^2\psi}{\partial T\partial m_{sk}}; \quad \frac{\partial\zeta}{\partial m_{sk}} = \frac{\partial A_m}{\partial\chi} = -\frac{\partial^2 U}{\partial\chi\partial m_{sk}} \quad (5a,b)$$

The first relation accounts for the latent heat effects related to the dehydration, and the second for the dependence of the hardening force ζ on hydrate mass m_{sk}. In view of (5), the state equations (4) are obtained upon differentiation in the following incremental form:

$$d\boldsymbol{\sigma} = \mathbf{C}:(d\boldsymbol{\varepsilon} - d\boldsymbol{\varepsilon}^p) + \mathbf{A}dT + \mathbf{B}dm_{sk} \quad (6)$$

$$T_0 dS = C_\varepsilon dT - T_0\mathbf{A}:(d\boldsymbol{\varepsilon} - d\boldsymbol{\varepsilon}^p) - ldm_{sk} \quad (7)$$

$$d\zeta = kdm_{sk} - hd\chi \quad (8)$$

$$dA_m = -\mathbf{B}:(d\boldsymbol{\varepsilon} - d\boldsymbol{\varepsilon}^p) - l\frac{dT}{T_0} + kd\chi - \kappa dm_{sk} \quad (9)$$

THERMAL DAMAGE AND THERMAL DILATATION

Eq. (6) can be inverted to read

$$d\boldsymbol{\varepsilon} = \boldsymbol{\Lambda}:d\boldsymbol{\sigma} + d\boldsymbol{\varepsilon}^p + \boldsymbol{\alpha}dT + \boldsymbol{\beta}dm_{sk} \quad (10)$$

In this equation

- $\boldsymbol{\Lambda}$ = fourth-order elastic compliance tensor, representing the inverse of the elastic tangential stiffness tensor $\mathbf{C} = \partial^2\psi/\partial\boldsymbol{\varepsilon}^2$ (tangent with respect to strain $\boldsymbol{\varepsilon}$). From a purely phenomenological view, this tensor is generally assumed to be a function of temperature T, as suggested by experiments [Fig. 1(a)]. Except for thermal damage induced by the difference in thermal dilatation coefficient between the (silicious) aggregates and the cement paste, this thermal damage cannot be regarded on the microlevel of material description as an actual change of the mechanical properties of the matter constituting concrete with temperature, but rather as a change in the concentration and structure of the cement paste constituents due to dehydration [e.g., Lin et al. (1996)]. On the macroscale of engineering material modeling, this can be considered through a dependence of the elastic material properties on the hydrate mass m_{sk} [i.e., $\mathbf{C} = \mathbf{C}(m_{sk})$], which constitutes a second-order chemomechanical cross-effect, as discussed later. In the isotropic case, the elastic stiffness tensor reads

$$\mathbf{C}(m_{sk}) = K(m_{sk})\mathbf{1}\otimes\mathbf{1} + 2G(m_{sk})\left(\mathbf{I} - \frac{1}{3}\mathbf{1}\otimes\mathbf{1}\right) \quad (11)$$

where $K(m_{sk}) = E(m_{sk})/3(1 - 2\nu)$ = bulk modulus; $G(m_{sk}) = E(m_{sk})/2(1 + \nu)$ = shear modulus; $\mathbf{1}$ = second-order unit tensor; $\mathbf{I}$ = fourth-order unit tensor; and

$$\boldsymbol{\Lambda}(m_{sk}) = \frac{1 + \nu}{E(m_{sk})}\mathbf{I} - \frac{\nu}{E(m_{sk})}\mathbf{1}\otimes\mathbf{1} \quad (12)$$

where $E(m_{sk})$ = Young's modulus; and ν = Poisson's ratio. The link between the elastic modulus E of concrete, mortar, and cement pastes, and the hydration products has been a matter of research for quite some time, namely in the context of experimental research on early-age concrete properties [e.g., Mindess et al. (1978), Byfors (1980), Laube (1990), Torrenti (1992), and Boumiz et al. (1996)]. These studies revealed a proportionality between the volume of hydration products and the elastic properties beyond the percolation threshold, i.e., $dE(m_{sk})/dm_{sk}$ = const. [see also Fig. 2 in Ulm and Coussy (1996)]. This proportionality can be considered as an intrinsic property of cement-based materials. It is assumed to hold also in the case of dehydration.
- $\mathbf{A} = \partial^2\psi/\partial\boldsymbol{\varepsilon}\partial T$ in (6) = compressive stress per unit change of temperature T induced by restrained thermal dilatation, and $\boldsymbol{\alpha} = -\boldsymbol{\Lambda}:\mathbf{A}$ in (10) = tensor of thermal dilatation coefficients, which (in the isotropic case) reduces to $\boldsymbol{\alpha} = \alpha\mathbf{1}$. The thermal dilatation coefficient depends mainly on the type of aggregate in concrete. Concretes with calcareous aggregates ($\alpha = 6-7 \times 10^{-6}$/K) have shown a decrease of thermal dilatation with temperature increase, while concretes with silicious aggregates are little affected by high temperatures ($\alpha = 12-13 \times 10^{-6}$/K).
- $\mathbf{B} = \partial^2\psi/\partial\boldsymbol{\varepsilon}\partial m_{sk}$ in (6) and $\boldsymbol{\beta} = -\boldsymbol{\Lambda}:\mathbf{B}$ in (10) are second-order tangential coupling tensors (tangent with respect to hydrate mass m_{sk}), and constitute the counterpart of the aforementioned chemomechanical coupling between the elastic properties and hydrate mass m_{sk}. Furthermore, tensor $\mathbf{B}$ may allow for the account of a chemical dilatation behavior (Coussy and Ulm 1996) related in concrete at high temperatures to the volume increase due to chemical transformation of the aggregates beyond 600–700°C [e.g., Lin et al. (1996)]. However, limiting the analysis to the temperature range that occurred during the Chunnel fire, this term will not be considered in the sequel. Thus, the assumed linear order of this coupling implies $\mathbf{B} = \boldsymbol{\sigma}/m_{sk}$, which satisfies the higher-order Maxwell-symmetry on elastic potential ψ (i.e., $\partial\mathbf{C}(m_{sk})/\partial m_{sk} = \partial\mathbf{B}/\partial\boldsymbol{\varepsilon} = \partial^3\psi/\partial\boldsymbol{\varepsilon}^2 m_{sk}$).

THERMAL DECOHESION AS CHEMOPLASTIC SOFTENING

The irreversible skeleton changes associated with microcracking are considered here within the framework of chemoplasticity (Coussy and Ulm 1996). This framework is a natural extension of the standard plasticity theory to chemoplastic couplings. As in standard plasticity, the plastic admissible stress states are defined by the loading function $f = f(\boldsymbol{\sigma}, \zeta)$, such that

$$\boldsymbol{\sigma} \in D_E \Leftrightarrow f(\boldsymbol{\sigma}, \zeta) \leq 0 \tag{13}$$

where D_E = elasticity domain; and ζ = hardening force, defined by (4*c*), which describes the strength domain of the material during chemoplastic evolution. In contrast to the standard plastic model, the latter depends not only on the plastic hardening/softening variable χ, but also on the hydrate mass m_{sk}:

$$d\zeta = k dm_{sk} - h d\chi \Leftrightarrow \zeta = \zeta(\chi, m_{sk}) \tag{14}$$

Note the difference with standard thermoplasticity models for concrete at elevated temperature, in which temperature dependent yield criteria are employed [e.g., Khennane and Baker (1992) and Heinfling et al. (1997)]. Considering that the dehydration is the main source of the macroscopically observable strength loss of rapidly heated concrete, the strength domain of concrete, expressed by the hardening force ζ, does not intrinsically depend on the temperature T (which corresponds to thermal hardening/softening), but rather on the hydrate mass m_{sk}. This is the phenomenon of chemical softening. It may be explained as follows (cf. Fig. 3): On the microlevel, the dehydration process can be roughly attributed to a microdiffusion of chemically bound water molecules from the micropores to the capillary pores. The loss of bound water, together with the chemical decomposition and dissociation of the hydration products, weakens the chemical bond structure of cement gel and destroys the cohesive forces in the micropores. On the macroscale of engineering material modeling, these phenomena lead to chemical softening, affecting the strength domain and its evolution, as expressed by (14). The effect of chemical softening is twofold: it affects the initial material threshold of the onset of plastic deformation (i.e., causes strength loss), as well as the plastic (hardening/softening) properties during irreversible skeleton deformation, characterized by

- $k = -\partial^2 U/\partial\chi\partial m_{sk}$, the chemoplastic coupling coefficient
- $h = \partial^2 U/\partial\chi^2$, the plastic hardening coefficient

They both derive from the frozen energy $U = U(\chi, m_{sk})$ associated with chemoplastic hardening/softening phenomena in the material.

For the evolution of the plastic variables, standard expressions can be applied for both the flow rule and the hardening rule. In particular, assuming associated plasticity, they read

$$d\boldsymbol{\varepsilon}^p = d\lambda \frac{\partial f(\boldsymbol{\sigma}, \zeta)}{\partial \boldsymbol{\sigma}}; \quad d\chi = d\lambda \frac{\partial f(\boldsymbol{\sigma}, \zeta)}{\partial \zeta} \tag{15a,b}$$

where $d\lambda(\geq 0)$ = plastic multiplier. It is obtained from the consistency condition $df = 0$ as (Coussy and Ulm 1996)

$$d\lambda = \frac{1}{H}\left[\frac{\partial f}{\partial \boldsymbol{\sigma}}:d\boldsymbol{\sigma} + \frac{\partial f}{\partial \zeta} k dm_{sk}\right] \tag{16}$$

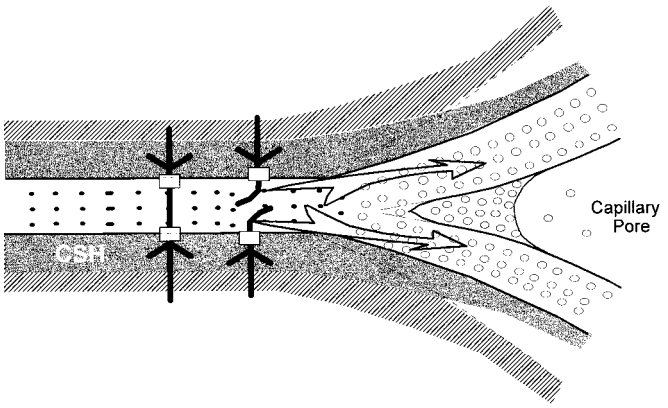

FIG. 3. Dehydration Sketch: Microdiffusion of Chemically Bound Water Molecules from Micropores to Capillary Pores

$$H = -\frac{\partial f}{\partial \zeta}\frac{\partial \zeta}{\partial \chi}\frac{d\chi}{d\lambda} = h\left(\frac{\partial f}{\partial \zeta}\right)^2 \tag{17}$$

where H = plastic hardening modulus, consistent with the standard definition of the sign of hardening modulus H (positive for plastic hardening, negative for plastic softening). Finally, as in standard plasticity, the associativity of both the flow and hardening rules assures the nonnegativity of the intrinsic energy dissipation rate φ_1 associated with irreversible skeleton deformations, i.e. (3*b*):

$$\varphi_1 dt = d\lambda\left(\boldsymbol{\sigma}:\frac{\partial f}{\partial \boldsymbol{\sigma}} + \zeta\frac{\partial f}{\partial \zeta}\right) \geq 0 \quad \text{if: } f = df = 0 \tag{18}$$

provided the loading function $f = f(\boldsymbol{\sigma}, \zeta)$ is convex with respect to its arguments, the stress $\boldsymbol{\sigma}$ and the hardening force ζ.

LATENT HEAT OF DEHYDRATION

Neglecting the external volume heat sources, the heat balance equation reads

$$T_0 \dot{S} = -\mathrm{div}\mathbf{q} + \varphi \tag{19}$$

where $\mathbf{q}$ = heat flux vector. The previous equation states that the internal entropy rate, $\dot{S}$, is equal to the sum of the entropy rate produced from the heat from the exterior (the term $-\mathrm{div}\mathbf{q}/T_0$) and the rate of internal entropy production due to dissipation [the term $\varphi/T_0 = (\varphi_1 + \varphi_c)/T_0$ given by (3)]. Then, using (7) in (19), one gets

$$C_\varepsilon \dot{T} + 3K\alpha T_0(\dot{\varepsilon} - \dot{\varepsilon}^p) - l\dot{m}_{sk} = -\mathrm{div}\mathbf{q} + \varphi \tag{20}$$

in which

- $C_\varepsilon = -T_0\partial^2\psi/\partial T^2$ = volume heat capacity of concrete (i.e., the heat per unit volume required for a unit temperature change).
- $3K\alpha T_0 = -T_0\partial^2\psi/\partial T\partial(\varepsilon - \varepsilon^p)$ = latent heat per unit of (elastic) volume deformation (with $\varepsilon = \mathrm{tr}\boldsymbol{\varepsilon}$ and $\varepsilon^p = \mathrm{tr}\boldsymbol{\varepsilon}^p$), and constitutes the counterpart of the aforementioned thermomechanical coupling of thermal dilatation. In an adiabatic experiment, this coupling in concretes may lead to a temperature change of $3K\alpha T_0/C_\varepsilon \approx -50$ to -80K per unit of elastic volume change (temperature increase in compression, temperature decrease in tension). In other words, with respect to the small order of magnitude of elastic volume strain in cementious materials ($|\varepsilon - \varepsilon^p| < 0.001$), this coupling may be considered as negligible as far as the heat equation is concerned.
- $l = T_0\partial^2\psi/\partial T\partial m_{sk}$ represents, with the opposite sign, the latent heat of dehydration per unit of hydrate mass m_{sk}. For $l > 0$ and $\dot{m}_{sk} < 0$ during dehydration, the latter appears in heat equation (20) as a sink term of volume heat, and corresponds to the endothermal nature of the dehydration process [e.g., Lin et al. (1996)]. This heat sink opposes the heat production related to the plastic energy dissipation, $\varphi_1 \geq 0$ according to (3*b*), and to energy dissipation by dehydration, $\varphi_c \geq 0$ according to (3*c*). Note, however, that the internal heat production in cementious materials due to energy dissipation is quite small. In an adiabatic experiment, $\varphi_1 dt/C_\varepsilon$ does not exceed about 10 to 20 K per unit of permanent strain (always positive due to the second law). With respect to their low ductility, this heat source (due to energy dissipation) can be considered as negligible in cementious materials.

Finally, for heat conduction, a linear law (Fourier law) may be adopted, i.e., $\mathbf{q} = -\mathcal{K}\mathrm{grad}T$, with $\mathcal{K}$ = conductivity. Neglecting the latent heat of (elastic) deformation and the heat

source due to energy dissipation, the heat equation (20) becomes

$$C_\epsilon \dot{T} = \mathcal{K}\nabla_{\mathbf{x}}^2 T + l\dot{m}_{sk} \tag{21}$$

where $\nabla_{\mathbf{x}}^2$ = Laplacian operator with respect to position vector $\mathbf{x}$.

DEHYDRATION KINETICS

As for the plastic deformations, a complementary evolution law for the dehydration process needs to be formulated. According to standard thermodynamics, it relates the driving force (i.e., affinity A_m) to the rate $\dot{m}_{sk}$. More precisely, if one considers the microdiffusion of water molecules from the micropores to the capillary pores as the rate determining process, $\dot{m}_{sk}$ is a diffusion rate that depends on the potential difference between the water in the micropores and that in the capillary pore space. At the macrolevel of material modeling, this potential difference is expressed by affinity A_m, and a discrete form of Fick's law can be adopted:

$$A_m = \eta \frac{dm_{sk}}{dt} \exp\left(\frac{E_a}{RT}\right) \tag{22}$$

where η = coefficient related to the microdiffusion; E_a = activation energy; and R = universal gas constant. The Arrhenius term $\exp(E_a/RT)$ accounts for the fact that the reaction in the micropore space occurs faster the higher the temperature. Furthermore, affinity A_m, which expresses the thermodynamic imbalance between the water molecules in the cement gel and those in the macropores, is given by (9).

Eq. (9) shows the counterparts of the chemomechanical, chemothermal, and chemoplastic couplings, with

- $\mathbf{B} = \partial^2\psi/\partial(\boldsymbol{\varepsilon} - \boldsymbol{\varepsilon}^p)\partial m_{sk}$ represents the thermodynamic imbalance induced by a unit strain change, and constitutes the chemomechanical counterpart of the dependence of the elastic properties on hydrate mass m_{sk}. Upon integration, this coupling term leads to second-order strain terms, which, in the hypothesis of infinitesimal strains (i.e., $\|\boldsymbol{\varepsilon}\| << 1$), can be neglected [e.g., Coussy and Ulm (1996)]. This leads one to assume that the dehydration process is not affected by macroscopic stress application (because $\mathbf{B} = \boldsymbol{\sigma}/m_{sk}$).
- $l/T_0 = \partial^2\psi/\partial T\partial m_{sk}$ represents the thermodynamic imbalance induced by a unit temperature change, the thermochemical counterpart of the latent heat of dehydration. While negligible for small temperature variations under typical ambient conditions [e.g., Ulm and Coussy (1996)], this coupling plays an important role in the dehydration of concrete in high temperatures.
- $k = -\partial^2 U/\partial\chi\partial m_{sk}$ represents the thermodynamic imbalance related to plastic hardening/softening phenomena, i.e., to microcracking, which can lead to dehydration. Yet, this effect of cracking on the hydration and dehydration process seems negligible, in particular with respect to the dehydration induced by thermochemical couplings.
- $\kappa = \partial^2 U/\partial m_{sk}$ is an equilibrium constant of the dehydration process considered.

Consider now an experiment in which a sudden temperature rise $T-T_0$ is imposed. Assuming chemoelastic evolutions and retaining only first-order terms, (22) and (9) yield

$$A_m = -\frac{l}{T_0}(T - T_0) + \kappa(m_0 - m_{sk}) = \eta \frac{dm_{sk}}{dt} \exp\left(\frac{E_a}{RT}\right) \tag{23}$$

where m_0 = initial hydration mass [i.e., $m_{sk}(0) = m_0$] at reference temperature $T = T_0$. The temperature rise $T-T_0$ induces a thermodynamic imbalance ($A_m < 0$), which drives dehydration $\dot{m}_{sk} < 0$ until thermodynamic equilibrium is reached (i.e., $A_m = 0$). From (23), it follows that

$$A_m = 0: \quad \xi(T) = \frac{m_{sk}}{m_0} = 1 - \frac{l/T_0}{\kappa m_0}(T - T_0) \tag{24}$$

where ξ = degree of hydration, as defined in cement chemistry (Powers and Brownyard 1948). In the approximate linear model developed here, the hydration degree ξ decreases linearly with increasing temperature, $T-T_0$. Moreover, because the dehydration is bound from below by $\xi = 0$ (which corresponds to complete dehydration), (24) indicates the maximum admissible temperature rise:

$$\xi = 0: \quad \max(T - T_0) = \frac{\kappa m_0}{l/T_0} \tag{25}$$

The latter depends on the initial hydrate mass, m_0, which in turn depends on the concrete mix ratios (for instance, the water/cement ratio). Finally, assuming η to be constant, the evolution of hydration degree ξ in the experiment considered reads

$$\xi(t) = \xi(T)\left[1 - \exp\left(-\frac{t}{\tau_d}\right)\right] \tag{26}$$

where $\xi(T)$ is the asymptotic solution (24), while

$$\tau_d = \frac{\eta}{\kappa} \exp\left(\frac{E_a}{RT}\right) \tag{27}$$

is the characteristic time of dehydration, which decreases with increasing temperature. The latter can be seen as a characteristic time of the microdiffusion between the micropores and the capillary space. It can be roughly estimated that $\tau_d \leq 5$ min at 20°C, $\tau_d \leq 10^{-1}$ s at 300°C, and $\tau_d \leq 10^{-3}$ s at 700°C (cf. Appendix I).

In the experiment considered, the temperature rise has been assumed to occur instantaneously compared to the microdiffusion of the dehydration process. This is not the case when considering the transport of heat by conduction through a structure, where the time and length scales of the dehydration reaction need to be seen in relation to the time and length scales of the heat transport in the structure. To this end, the dimensionless variables are introduced in both the spatial coordinate $\mathbf{X} = \mathbf{x}/\mathcal{L}$ and the time coordinate $s = t/\mathcal{T}$ in heat equation (21):

$$\frac{\partial T}{\partial s} = \nabla_{\mathbf{X}}^2 T + l/C_\epsilon \frac{\partial m_{sk}}{\partial s} \tag{28}$$

and in kinetics law (23):

$$\frac{A_m}{\kappa} = -\frac{l}{\kappa T_0}(T - T_0) + m_0 - m_{sk} = \frac{\tau_d}{\mathcal{T}} \frac{\partial m_{sk}}{\partial s} \tag{29}$$

where $\nabla_{\mathbf{X}}^2$ = Laplacian operator with respect to the dimensionless space variable $\mathbf{X}$; and $\mathcal{T}$ = characteristic time of the heat conduction, which is usually related to the characteristic length $\mathcal{L}$ by

$$\mathcal{T} = \frac{\mathcal{L}^2}{\mathcal{K}/C_\epsilon} \tag{30}$$

Eq. (29) gives an insight into the concept of thermodynamic equilibrium of the dehydration process coupled with heat conduction in the structure. In fact, if one considers $\tau_d/\mathcal{T} \to 0$, (29) yields

$$\frac{\tau_d}{\mathcal{T}} \to 0 \Rightarrow A_m = 0: \quad \xi = \xi(T) \tag{31}$$

which turns out to be the condition of thermodynamic equi-

librium, i.e., (24). Furthermore, if $\tau_d << \mathcal{T}$, the dehydration process can be considered as (almost) terminated for an observation length scale satisfying the condition

$$\tau_d << \mathcal{T} \Leftrightarrow \mathcal{L} >> \sqrt{\tau_d \mathcal{H}/C_\varepsilon} \tag{32}$$

This is generally the case when considering as the observation length scale the structural scale of heat conduction. In fact, a rough estimation of the right-hand side of inequality (32) for rapidly heated concrete under fire conditions with temperature rises of $T - T_0 = 300-700$ K (Appendix I) gives $\sqrt{\tau_d \mathcal{H}/C_\varepsilon} \approx 10^{-4}$ m at 300°C, and $\sqrt{\tau_d \mathcal{H}/C_\varepsilon} \approx 10^{-5}$ m at 700°C, which is several orders of magnitudes smaller than the typical scale of heat conduction in concrete structures.

In other words, (24), (29), and (31) reveal the existence of a unique thermal dehydration function $\xi = \xi(T)$, obtained from thermodynamic equilibrium relative to the time and length scales of structural heat transport involved in chemoelastic evolutions. This still holds in chemoplastic evolutions, provided that the effect of microcracking on affinity A_m [i.e., the term $kd\chi$ in (9)] is negligible with respect to the dehydration induced by thermochemical couplings. This partial decoupling hypothesis reads formally

$$\forall \chi \quad \text{and} \quad \tau_d << \mathcal{T}: \quad \xi = \xi(T) \tag{33}$$

EXPERIMENTAL IDENTIFICATION OF THERMAL DEHYDRATION FUNCTION

In the preceding paragraph, the thermal dehydration function (24) has been theoretically derived as an asymptotic solution of the dehydration process under the hypothesis of a linear dependence of affinity A_m on temperature T and hydrate mass m_{sk} [i.e., (23)]. This hypothesis deserves verification. For a given temperature rise $T-T_0$, the hydration degree ξ needs to be determined experimentally. Alternatively, the evolution of the hydration degree can be followed indirectly through the effects of dehydration, namely through the cross-effects with the changes in elastic stiffness (thermal damage) or in material strength (thermal decohesion).

To this end, consider the linear chemomechanical coupling $E(\xi) = E_0\xi$, which expresses (in the isotropic case) the proportionality between the volume of hydration products and the elastic properties of concrete. The proportionality has been found to constitute an intrinsic material property of concrete. It is assumed to hold as well in the case of dehydration, with E_0 the elastic modulus for $\xi = 1$. Furthermore, the thermal damage of rapidly heated concrete is generally described in terms of experimentally determined relations $E = E(T)$, which link the temperature T to the elastic modulus E [Fig. 1(a)]. Then, combining this phenomenological relation, $E = E(T)$, with the aforementioned intrinsic proportionality, $E(\xi) = E_0\xi$, one can determine the thermal dehydration function

$$\xi(T) = \frac{E(T)}{E_0} \tag{34}$$

This equation is plotted in Fig. 4 for the concrete of the Chunnel. The values for $E(T)$ have been obtained by Fasseu (1997) on cored cylindrical specimens of undamaged concrete of the chunnel rings. These specimens were cut in slices of diameter 73.5 mm and 8 mm thickness, and subject to different controlled furnace temperature rises varying from 100 to 700°C. After cooling, the elastic modulus was determined by dynamic measurements and compared to the initial dynamic modulus of $E_0 = 46$ MPa [for preparation, and the devices for testing, see Fasseu (1997)]. The thermal dehydration function $\xi = \xi(T)$, determined according to (34), shows a pronounced proportional decrease in the hydration degree with temperature in the range of $T-T_0 \in [0; 600]$ K. This confirms the assumed linearity of affinity A_m with respect to temperature and hydrate mass, and shows how the macroscopic thermal dehydration function $\xi = \xi(T)$ can be determined from the apparent temperature dependence of the mechanical material properties of rapidly heated concrete, provided that the degree of the chemomechanical coupling (i.e., the dependence on hydration degree ξ) is known.

Furthermore, the thermal dehydration function $\xi = \xi(T)$ may partly explain the temperature dependence of the apparent volume heat capacity of concrete. Its value has been found to increase with temperature T [e.g., Franssen (1987) and Noumowé (1995)]. The asymptotic solution to the dehydration process, $\xi = \xi(T)$, according to (24), in (21), yields the heat equation in the form

$$C_{\tau_d/\mathcal{T}\to 0}\dot{T} = K\nabla_x^2 T \tag{35a}$$

$$C_{\tau_d/\mathcal{T}\to 0} = C_\varepsilon - lm_0\frac{d\xi}{dT} = C_\varepsilon + l^2/(T_0\kappa) \tag{35b}$$

where $C_{\tau_d/\mathcal{T}\to 0}$ = apparent volume heat capacity. Note the increase in the apparent heat capacity due to the ''heat sink'' of dehydration (i.e., $C_{\tau_d/\mathcal{T}\to 0} \geq C_\varepsilon$). In the simplified linear model developed here (in which affinity A_m is linear with respect to temperature T and hydrate mass m_{sk}), this increase is constant. Fig. 5 compares the apparent heat capacity determined from

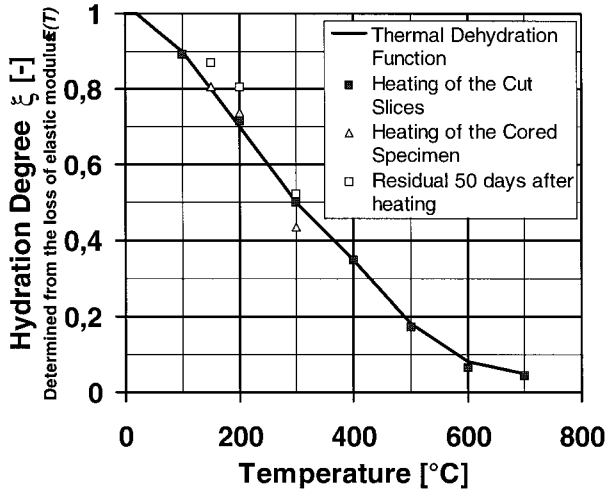

FIG. 4. Thermal Dehydration Function $\xi = \xi(T)$, Determined from Thermal Loss of Elastic Stiffness $E = E(T)$ of Chunnel Concrete [Experimental Data from Fasseu (1997)]

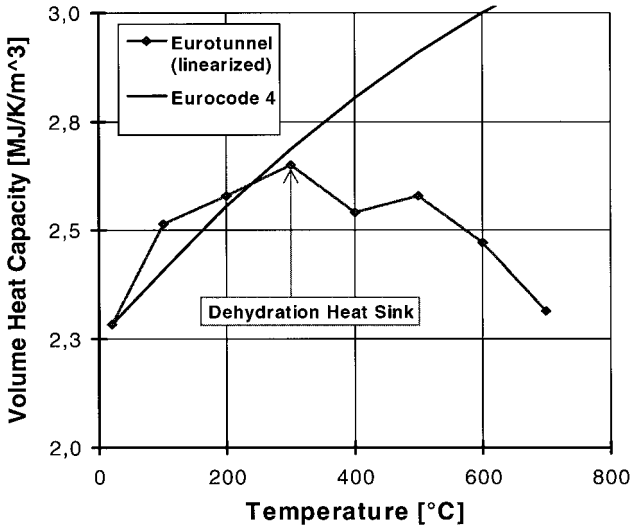

FIG. 5. Temperature Dependence of Apparent Volume Heat Capacity of Concrete according to Eq. (35*b*) Obtained for Chunnel Concrete and to Eurocode 4 (''Conception'' 1994)

(35*b*) using the thermal dehydration function $\xi = \xi(T)$ of Fig. 4, with the typical apparent temperature dependence considered in international design codes (''Conception'' 1994). In the general nonlinear case, a monotonic increase of heat capacity $C_{\tau_d/\mathcal{T}\to 0}$ with temperature could be obtained. However, as shown by the preceding dimensional analysis, this empirical temperature dependence is not an intrinsic material property (i.e., independent of boundary conditions, specimen size, etc.), but is related through the characteristic time ratio $\tau_d/\mathcal{T}$ to the time and length scales of the structural heat transport.

WILLAM-WARNKE CRITERION WITH ISOTROPIC CHEMOPLASTIC SOFTENING

By way of application, the model for chemoplastic softening will now be combined with the three-parameter Willam-Warnke yield criterion. For the sake of clarity, isotropy will be assumed for both chemical and plastic hardening or softening. Willam and Warnke's (1975) loading function of plasticity reads

$$f = \tau + \delta(\theta)(\sigma - \rho(\chi, \xi)) \tag{36}$$

where (τ, θ, σ) = invariants of stress tensor $\boldsymbol{\sigma} = \mathbf{s} + \sigma\mathbf{1}$ with eigenvalues $\sigma_1 \geq \sigma_2 \geq \sigma_3$, and $\mathbf{s}$ = stress deviator:

$$\tau = \sqrt{\frac{1}{2}\mathbf{s}:\mathbf{s}}; \quad \sigma = \frac{1}{3}tr\sigma; \quad \cos\theta = \frac{2\sigma_1 - \sigma_2 - \sigma_3}{\sqrt{12}\tau} \tag{37a–c}$$

Furthermore, $\delta(\theta)$ = friction angle, which depends on Lode angle θ varying between friction coefficient $\delta_t = \delta(\theta = 0°)$ on the tensile meridian and friction coefficient $\delta_c = \delta(\theta = 60°)$ on the compressive meridian (Fig. 6). The expression for $\delta(\theta)$ can be found in many textbooks [cf. Chen and Han (1988)], and is given in Appendix II. Finally, $\rho = \rho(\chi, \xi)$ is the cohesion pressure, which, for the present isotropic chemoplastic hardening, depends on the hardening variable χ and the hydration degree ξ. In the ideal plastic case (i.e., $\rho = \rho_0$), the three material parameters, i.e., the cohesive pressure ρ_0 and friction coefficients δ_t and δ_c, are related to the standard material characteristics by

$$f_c = \frac{3\delta_c}{\sqrt{3} - \delta_c}\rho_0; \quad f_t = \frac{3\delta_t}{\sqrt{3} - \delta_t}\rho_0; \quad f_{bc} = \frac{3\delta_t}{\sqrt{3} - 2\delta_t}\rho_0 \tag{38a–c}$$

where f_c = uniaxial compressive strength; f_t = uniaxial tensile strength; and f_{bc} = biaxial compressive strength. The extension to chemoplastic hardening/softening is straightforward—it suffices to replace in relations (38) ρ_0 by $\rho = \rho(\chi, \xi)$. More precisely, the line of argument is as follows:

1. $f_c = f_c(\xi)$ is an intrinsic material function. The dependence of the material strength on the solidified material volume (proportional to ξ) has a mechanical meaning. This cannot a priori be said about the phenomenological relation $f_c = f_c(T)$, when setting the phenomenon of thermal microcracking due to the difference in thermal dilatation coefficient aside (a reasonable assumption in particular in the case of concretes with calcareous aggregates).
2. $\xi = \xi(T)$ is a thermodynamic equilibrium condition (i.e., $A_m = 0$), and defines a dehydration *state*.
3. Combining the two previous points, i.e., $f_c = f_c(\xi)$ and $\xi = \xi(T)$, yields $f_c(T) = f_c(\xi(T))$. In other words, the combination of the mechanical meaning of $f_c = f_c(\xi)$ and the thermodynamic equilibrium condition $\xi = \xi(T)$ gives a mechanical and a thermodynamic interpretation of the empirical relation $f_c = f_c(T)$ accessible by standard material tests [cf. Fig. 1(b)]. Thus, provided the thermodynamic equilibrium condition $\xi = \xi(T)$, chemoplasticity reduces to thermoplasticity, and chemical damage to thermal damage. The same line of argument has been applied to determine the thermal dehydration function from the apparent thermal damage, $E = E(T)$ of the chunnel concrete [i.e., (34)].

Since the compressive strength of concrete has been found to decrease almost linearly with the temperature, the following expression can be adopted for the case of isotropic chemoplastic hardening/softening in the context of the three-parameter chemoplastic Willam-Warnke yield criterion:

$$\rho(\chi, \xi) = \xi z(\chi)\rho_0 \tag{39}$$

where $z(\chi) \in [0; 1]$ denotes a suitable expression for the plastic hardening/softening in hardened concrete.

Next, assuming associated plasticity, the flow rule (15*a*) reads

$$d\boldsymbol{\varepsilon}^p = d\mathbf{e}^p + \frac{1}{3}d\varepsilon^p\mathbf{1} \tag{40a}$$

$$d\mathbf{e}^p = d\lambda(\mathbf{s}/2\tau + (\sigma - \xi z(\chi)\rho_0)\mathbf{P}); \quad d\varepsilon^p = tr(d\boldsymbol{\varepsilon}^p) = d\lambda\delta(\theta) \tag{40b,c}$$

where $\mathbf{P} = \partial\delta(\theta)/\partial\boldsymbol{\sigma}$, the expression of which is given in Appendix II. Concerning the hardening law, the plastic volume dilatation is considered as the hardening variable, i.e., $\chi = \varepsilon^p$.

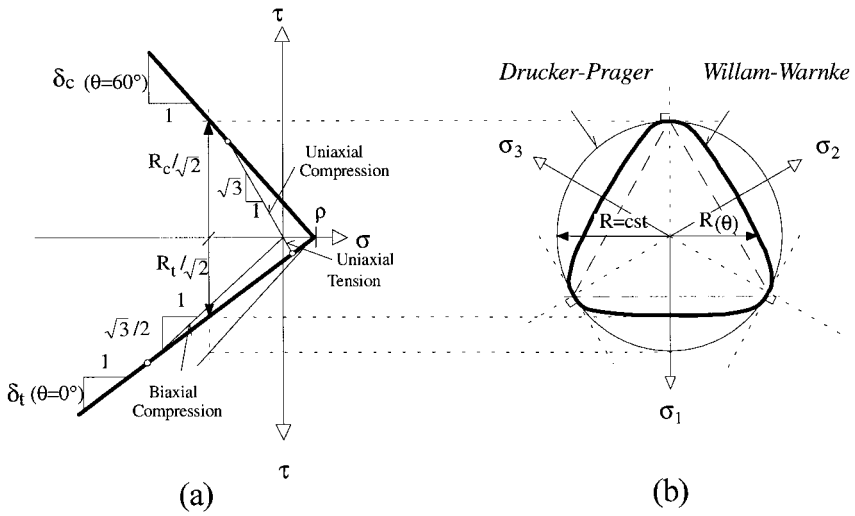

FIG. 6. Three Parameter Willam-Warnke Criterion: (a) in (τ, σ)-Half-Spaces of Compressive and Tensile Meridians; (b) in Deviator Plane

In the context of an associated hardening rule (15*b*), this choice implies the following expression for the hardening force $\zeta = \zeta(\chi, \xi)$ in the yield criterion (36):

$$f(\boldsymbol{\sigma}, \zeta) = \tau + \delta(\theta)(\sigma - \rho_0 + \zeta) \tag{41}$$

$$\zeta(\chi = \varepsilon^p, \xi) = \rho_0[1 - \xi z(\chi = \varepsilon^p)] \tag{42}$$

Using (41) in (15*b*) yields

$$d\chi = d\lambda \frac{\partial f(\boldsymbol{\sigma}, \zeta)}{\partial \zeta} = d\lambda \delta(\theta) \tag{43}$$

which is equal to the incremental plastic dilatation $d\varepsilon^p$ given by the flow rule (40*c*).

Finally, (16), (17), (40), and (43) yield the hardening modulus H and the plastic multiplier $d\lambda$ for the Willam-Warnke model with isotropic chemoplastic hardening:

$$H = h \left(\frac{\partial f}{\partial \zeta}\right)^2 = \xi h_0 \delta(\theta)^2 = \xi H_0 \tag{44}$$

$$d\lambda = \frac{1}{\xi H_0}[d\tau + \delta(\theta) d\sigma + (\sigma - \rho_0 + \zeta)\mathbf{P}:d\mathbf{s} + \delta(\theta)(\rho_0 - \zeta) d\xi/\xi] \tag{45}$$

where $h_0 = \rho_0 dz(\varepsilon^p)/d\varepsilon^p$ and H_0 = plastic hardening coefficient and hardening modulus of the material at $\xi = 1$. Note that the sign of the hardening modulus H is given by the sign of the plastic hardening coefficient $h_0 = h_0(\varepsilon^p)$ for the plastic hardening or softening behavior. In turn, with advancing dehydration, the material approaches the ideal plastic limit case ($H = 0$), which is obtained at complete dehydration ($\xi = 0$). This linear dependence of the plastic hardening and softening properties on the hydration degree ξ, however, still needs to be confirmed from experimental data on the hardening and softening of concrete at high temperatures [for instance, from fracture energy G_f, which is proportional to frozen energy $U(\chi, \xi)$ of chemoplastic hardening, from which—according to (4*c*)—hardening force ζ, i.e. (42), ensues]. Finally, the choice of the three-parameter Willam-Warnke yield criterion with isotropic chemoplastic hardening/softening is not restrictive. The same line of argument can be applied to any other loading function and hardening models.

CHEMOPLASTIC RETURN MAPPING ALGORITHM

Finally, some comments on the numerical treatment of the chemoplastic constitutive equations of the dehydration model in the constitutive library of finite-element program are in order. In the context of an Euler backward scheme, the discrete version of state equations (6) and (14) together with (42) reads (in the isotropic case)

$$\boldsymbol{\sigma}_{n+1} = \boldsymbol{\sigma}_n \frac{\xi_{n+1}}{\xi_n} + \frac{E_0 \xi_{n+1}}{1 + \nu}(\Delta\mathbf{e}_{n+1} - \Delta\mathbf{e}^p_{n+1}) + \frac{E_0 \xi_{n+1}}{3(1 - 2\nu)}(\Delta\varepsilon_{n+1} - \Delta\varepsilon^p_{n+1} - 3\alpha\Delta T_{n+1})\mathbf{1} \tag{46}$$

$$\zeta_{n+1} = \rho_0 + (\zeta_n - \rho_0)\frac{\xi_{n+1}}{\xi_n} - \xi_{n+1} h_0(\chi_{n+1})\Delta\chi_{n+1} \tag{47}$$

with $\Delta(\bullet)_{n+1} = (\bullet)_{n+1} - (\bullet)_n$, where subscripts $(\bullet)_n$ and $(\bullet)_{n+1}$ indicate the chemoplastic solutions for the preceding and the current time steps, t_n and t_{n+1}, respectively. In (46) and (47), $\Delta\boldsymbol{\varepsilon}_{n+1} = \Delta\mathbf{e}_{n+1} + (1/3)\Delta\varepsilon_{n+1}\mathbf{1}$ and ΔT_{n+1} are the finite increments of the external variables, obtained as a solution of the global balance equations (i.e., the momentum balance equation and heat balance equation). For the chemoplastic model at hand, advanced numerical tools of computational plasticity [e.g., Simo and Hughes (1997)] can be readily modified to accommodate chemoplasticity. In particular, the internal state variables at instant t_{n+1} (i.e., the plastic variables $\boldsymbol{\varepsilon}^p_{n+1}$ and χ_{n+1}, and the hydration degree ξ_{n+1}) are suitably updated by using a return mapping algorithm. The return mapping algorithm starts from a trial state (or predictor step), which indicates whether plastic flow occurs. In the standard plastic model, this predictor step is completely defined by the elastic trial stress $\boldsymbol{\sigma}^{\text{trial}}_{n+1}$. Because the elasticity domain in chemoplasticity may evolve independently of plastic deformations, as a function of hydration degree ξ (pure chemical hardening/softening), the trial state in chemoplasticity needs to take into account both the trial stress, $\boldsymbol{\sigma}^{\text{trial}}_{n+1}$, and the trial hardening force, $\zeta^{\text{trial}}_{n+1}$, as shown in Fig. 7 in the $(\boldsymbol{\sigma} \times \zeta)$-space. This chemoelastic predictor respects the standard format of computational plasticity (Hellmich et al. 1997):

$$f(\boldsymbol{\sigma}^{\text{trial}}_{n+1}, \zeta^{\text{trial}}_{n+1}) > 0 \Leftrightarrow \Delta\lambda_{n+1} > 0 \tag{48a}$$

$$f(\boldsymbol{\sigma}^{\text{trial}}_{n+1}, \zeta^{\text{trial}}_{n+1}) \leq 0 \Leftrightarrow \Delta\lambda_{n+1} = 0 \tag{48b}$$

and is obtained from (46) and (47) by freezing the plastic flow (i.e., $\Delta\boldsymbol{\varepsilon}^{p,\text{trial}}_{n+1} = 0$ and $\Delta\chi^{\text{trial}}_{n+1} = 0$):

$$\boldsymbol{\sigma}^{\text{trial}}_{n+1} = \boldsymbol{\sigma}_n \frac{\xi^{\text{trial}}_{n+1}}{\xi_n} + \frac{E_0 \xi^{\text{trial}}_{n+1}}{1 + \nu}\Delta\mathbf{e}_{n+1} + \frac{E_0 \xi^{\text{trial}}_{n+1}}{3(1 - 2\nu)}(\Delta\varepsilon_{n+1} - 3\alpha\Delta T_{n+1})\mathbf{1} \tag{49}$$

$$\zeta^{\text{trial}}_{n+1} = \rho_0 + (\zeta_n - \rho_0)\frac{\xi^{\text{trial}}_{n+1}}{\xi_n} \tag{50}$$

where ξ^{trial}_{n+1} represents the hydration degree under chemoelastic conditions given, according to (31), by the thermal dehydration function $\xi = \xi(T)$. In addition, the partial decoupling hypothesis (33) reads:

$$\xi_{n+1} = \xi^{\text{trial}}_{n+1} = \xi(T_{n+1}) \tag{51}$$

which expresses the assumption of a negligible effect of plastic hardening or softening on affinity A_m. This allows one, from an algorithmic point of view, to consider chemically inert conditions during the plastic corrector step: the hydration degree is not altered due to plastic flow. In other words, the return map involves only plastic flow, i.e., an (almost) standard projection of the trial state (49) and (50) onto the initially updated chemoplastic loading surface $f[\boldsymbol{\sigma}_{n+1}, \zeta(\xi_{n+1} = \xi^{\text{trial}}_{n+1}, \chi_{n+1})] = 0$. Such plastic return mapping algorithms can be found in standard textbooks on computational plasticity [e.g., Simo and Hughes (1997)]. In the case of the Willam-Warnke criterion, with its dependence on the Lode angle θ, an explicit return mapping algorithm [i.e., the cutting-plane algorithm proposed by Ortiz and Simo (1986)] is more suitable for determining the plastic admissible stress $\boldsymbol{\sigma}_{n+1}$ and hardening force ζ_{n+1} than

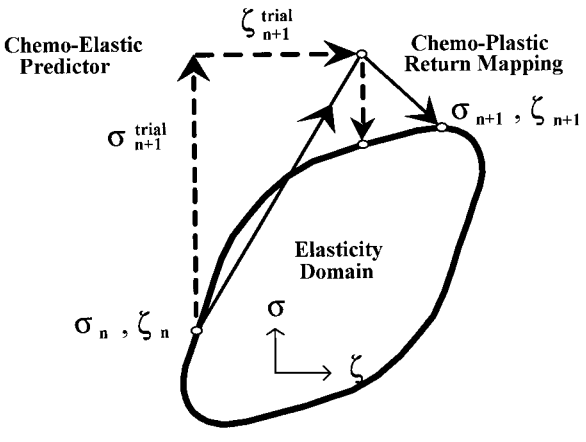

FIG. 7. Chemoelastic Trial State ($\boldsymbol{\sigma}^{\text{trial}}_{n+1}, \zeta^{\text{trial}}_{n+1}$) for Chemoplastic Return Mapping Algorithm in ($\boldsymbol{\sigma} \times \zeta$)-Space

the implicit closest-point projection algorithm, which requires second derivatives of the loading function.

CONCLUSIONS

The constitutive model for rapidly heated concrete presented in this paper considers the dehydration of concrete at high temperature and its coupling with temperature, elastic, and plastic deformations. It has the following characteristic features:

1. The apparent thermal damage and thermal decohesion result mainly from the dehydration of concrete at high temperature. This means that the mechanical material properties of rapidly heated concrete (Young's modulus, material strength) do not intrinsically depend on the temperature T, but rather on the hydration degree ξ. Set within the framework of chemoplasticity, this dependence on hydration degree ξ characterizes the chemomechanical couplings. In the case of rapidly heated concrete, the hydration is reversed to chemoplastic softening. Standard yield criteria for concrete can be readily adapted to take these phenomena into account. This is illustrated for the three-parameter Willam-Warnke criterion with isotropic chemoplastic softening. The implementation of the chemoplastic model for dehydration in the constitutive library of finite-element programs requires only minor modifications concerning the trial state in chemoplasticity.
2. The dehydration process is described by a kinetics law that relates the driving force (affinity A_m) to the dehydration rate. The thermodynamic imbalance induced by chemothermal coupling results in dehydration, until thermodynamic equilibrium is reached. A state function $\xi = \xi(T)$ can be derived to relate the temperature T to hydration degree ξ at thermodynamic equilibrium. From dimensional analysis of the heat equation, and the fact that the characteristic time of dehydration is much inferior to the characteristic time of structural heat conduction, it is shown that this thermal dehydration function $\xi = \xi(T)$ still applies when the heat transport in the structure is taken into account. The function $\xi = \xi(T)$ can be determined from available experimental data on rapidly heated concrete by exploring the chemomechanical couplings together with the empirical temperature dependence of the macroscopic material properties of concrete. This is shown for the experimentally determined temperature dependence of the elastic modulus of the concrete of the Chunnel rings. The results confirm a linear decrease of hydration degree ξ with the temperature rise.
3. For the sake of simplicity, the elementary system has been considered as closed with respect to the fluid phases saturating the macropore space. It could be argued that the time scale of fire duration (10 h) is much smaller than the time scale of the diffusion of water and vapor in the structure (which is due to the low permeability of concrete, i.e. 10^{-9} m/s for a low quality concrete, and 10^{-12} m/s for a high strength concrete), and that the role of the pore pressure on deformation, cracking and fracture in rapidly heated concrete is not yet clear (see the Introduction). However, this hypothesis, as well as the choice of plastic variables to represent cracking, should be seen in the perspective of the overall scope of this study, whose main aim is the evaluation of the risk of spalling due to restrained thermal dilatation as experienced in the Chunnel fire. This is analyzed in the companion paper (Ulm et al. 1999).

APPENDIX I. CHARACTERISTIC TIME OF DEHYDRATION

The order of magnitude of the characteristic time of dehydration, τ_d, can be roughly estimated by considering the microdiffusion between the micropores and the capillary pores, with an average diffusion length d traveled by the water molecules from the micropores to the capillary pores, and an average diffusivity D:

$$\tau_d \approx \tau_d(T_0)\exp\left[\frac{E_a}{R}\left(\frac{1}{T}-\frac{1}{T_0}\right)\right]; \quad \tau_d(T_0) \approx \frac{d^2}{D(T_0)} \qquad (52a,b)$$

where $D(T_0)$ = diffusivity of water passing through the pores at reference temperature, $D(T_0 = 293\ \text{K}) \approx 10^{-12}$ m^2/s; $2d$ = average distance between two macropores ($2d \approx 10-40$ μm); and $E_a/R \cong 5{,}000$ K. These values yield $\tau_d(T_0) = 25-400$ s; $\tau_d = 6-96 \times 10^{-3}$ s at 300°C; and $\tau_d = 17-265 \times 10^{-5}$ s at 700°C. The length scale, $\sqrt{\tau_d \mathcal{K}/C_\varepsilon}$, corresponding to these microdiffusion times, can be roughly estimated from the thermal conductivity $\mathcal{K} = 8$ kJ/h/m/K and a volume heat capacity $C_\varepsilon = 2{,}500$ kJ/m^3/K. One gets $\sqrt{\tau_d \mathcal{K}/C_\varepsilon} = 5-20$ mm at 20°C, $\sqrt{\tau_d \mathcal{K}/C_\varepsilon} = 70-290$ μm at 300°C, and $\sqrt{\tau_d \mathcal{K}/C_\varepsilon} = 10-50$ μm at 700°C.

APPENDIX II. WILLAM-WARNKE YIELD CRITERION

The expression of friction coefficient $\delta(\theta)$ as a function of Lode angle θ in the Willam-Warnke yield criterion is given by (Willam and Warnke 1975; Chen and Han 1988)

$$\delta(\theta) = \frac{u + v}{w} \qquad (53)$$

with

$$u = 2\delta_c(\delta_c^2 - \delta_t^2)\cos\theta$$

$$v = \delta_c(2\delta_t - \delta_c)\sqrt{4(\delta_c^2 - \delta_t^2)\cos^2\theta + 5\delta_t - 4\delta_c\delta_t}$$

$$w = 4(\delta_c^2 - \delta_t^2)\cos^2\theta + (\delta_c - 2\delta_t)^2$$

The convexity of yield criterion (41) with respect to its arguments, the stress tensor $\boldsymbol{\sigma}$ and the hardening force ζ, entails the following restrictions on friction coefficients δ_c and δ_t, independently of the chemoplastic couplings considered:

$$\frac{1}{2}\delta_t \le \delta_c \le 2\delta_t \qquad (54)$$

Furthermore, the very existence of the strength domain defined by (38) implies

$$0 \le \delta_c < \sqrt{3} \quad 0 \le \delta_c < \sqrt{3}/2 \quad \rho \ge 0 \qquad (55)$$

The derivative of function $\delta(\theta)$ with respect to the stress tensor $\boldsymbol{\sigma}$ reads

$$\mathbf{P} = \frac{\partial\delta(\theta)}{\partial\boldsymbol{\sigma}} = -\frac{\partial\delta(\theta)}{\partial(\cos\theta)}\frac{1}{2\sqrt{12\tau^3}}\mathbf{Q} \qquad (56)$$

where

$$\frac{\partial\delta(\theta)}{\partial(\cos\theta)} = \frac{(u' + v')w - (u + v)w'}{w^2} \qquad (57)$$

with

$$u' = 2\delta_c(\delta_c^2 - \delta_t^2); \quad v' = \frac{w'}{2v}\delta_c^2(2\delta_t - \delta_c); \quad w' = 8(\delta_c^2 - \delta_t^2)\cos\theta$$

and $\mathbf{Q}$ a second-order tensor of a zero trace, given by

$$\mathbf{Q} = (2\sigma_1 - \sigma_2 - \sigma_3)\mathbf{s} - 2\tau^2(2\mathbf{u}_1 \otimes \mathbf{u}_1 - \mathbf{u}_2 \otimes \mathbf{u}_2 - \mathbf{u}_3 \otimes \mathbf{u}_3) \qquad (58)$$

where ($\mathbf{u}_1$; $\mathbf{u}_2$; $\mathbf{u}_3$) = eigenvectors associated with the eigenvalues ($\sigma_1 \geq \sigma_2 \geq \sigma_3$) of stress tensor $\boldsymbol{\sigma}$.

ACKNOWLEDGMENTS

This study is part of the consulting mission of LCPC to SETEC TPI (Paris) on the repair of the Chunnel after the fire of November 18, 1996. The writers wish to thank Michel Lévy, director at SETEC TPI and project manager of the repair of the tunnel, for partial support of this research.

APPENDIX III. REFERENCES

Ahmed, G. N., and Hurst, J. P. (1995). ''Modeling the thermal behavior of concrete slabs subjected to the ASTM E119 standard fire conditions.'' *J. Fire Protection Engrg.*, 7(4), 125–132.

Anderberg, Y. (1997). ''Spalling phenomena of HPC and OC.'' *Proc., Int. Workshop on Fire Performance of High-Strength Concrete, NIST Spec. Publ. 919*, L. T. Phan, N. J. Carino, D. Duthinh, and E. Garboczi, eds., National Institute of Standards and Technology, Gaithersburg, Md., 69–73.

Bažant, Z. P. (1997). ''Analysis of pore pressure, thermal stresses and fracture in rapidly heated concrete.'' *Proc., Int. Workshop on Fire Performance of High-Strength Concrete, NIST Spec. Publ. 919*, L. T. Phan, N. J. Carino, D. Duthinh, and E. Garboczi, eds., National Institute of Standards and Technology, Gaithersburg, Md., 155–164.

Bažant, Z. P., and Kaplan, M. F. (1996). *Concrete at high temperatures: Material properties and mathematical models*, Longman (Addison-Wesley, London.

Bažant, Z. P., and Thongutai, W. (1978). ''Pore pressure and drying of concrete at high temperature.'' *J. Engrg. Mech. Div.*, ASCE, 104, 1058–1080.

Bažant, Z. P., and Thongutai, W. (1979). ''Pore pressure in heated concrete walls: Theoretical prediction.'' *Mag. of Concrete Res.*, London, 31(107), 67–76.

Boumiz, A., Vernet, C., and Cohen Tenoudji, F. (1996). ''Mechanical properties of cement pastes and mortars at early ages. Evolution with time and degree of hydration.'' *Advanced Cement Based Mat.*, 3, 94–106.

Byfors, J. (1980). ''Plain concrete at early ages.'' *Res. Rep. F3:80*, Swedish Cement and Concrete Research Institute, Stockholm.

Chen, W. F., and Han, D. J. (1988). *Plasticity for structural engineers*. Springer, New York.

''Conception et dimensionnement des structures mixtes acier-béton.'' *Eurocode 4*, AFNOR, Paris.

Consolazio, G. R., McVay, M., and Rish, J. W. III. (1997). ''Measurement and prediction of pore pressure in cement mortar subjected to elevated temperature.'' *Proc., Int. Workshop on Fire Performance of High-Strength Concrete, NIST Spec. Publ. 919*, L. T. Phan, N. J. Carino, D. Duthinh, and E. Garboczi, eds., National Institute of Standards and Technology, Gaithersburg, Md., 125–148.

Coussy, O. (1995). *Mechanics of porous continua*. Wiley, Chichester, U.K.

Coussy, O., and Ulm, F.-J. (1996). ''Creep and plasticity due to chemomechanical couplings.'' *Archive of Appl. Mech.*, 66, Springer, Berlin, 523–535.

Fasseu, P. (1997). ''Eurotunnel-Fire. Analysis of the effect of the fire on the concrete quality.'' *Res. Rep. No. 96.6002532 (April 1997)*, Laboratoire Regional des Ponts et Chaussées de Lille, Lille, France (in French).

Franssen, J. M. (1987). ''Analysis of the fire behavior of steel-concrete composite structures,'' PhD thesis, No. 111, University of Liège, Liège, Belgium (in French).

Harmathy, T. Z. (1965). ''Effect of moisture on the fire endurance of building materials.'' *No. 385*, ASTM, Philadelphia, 74–95.

Heinfling, G., Reynouard, J. M., Merabet, O., and Duval, C. (1997). ''A thermo-elastic-plastic model for concrete at elevated temperatures including cracking and thermo-mechanical interaction strains.'' *Computational Plasticity. Fundamentals of Applications (Proc. COMPLAS V)*, D. R. J. Owen, E. Onate, and E. Hinton, eds., Vol. 2, CIMNE, Barcelona, Spain, 1493–1498.

Hellmich, C., Ulm, F.-J., and Mang, H. A. (1997). ''Chemoplasticity for shotcrete at early ages.'' *Computational Plasticity. Fundamentals and Applications (Proc. COMPLAS V)*, D. R. J. Owen, E. Onate, and E. Hinton, eds., Vol. 2, CIMNE, Barcelona, Spain, 1499–1507.

Khennane, A., and Baker, G. (1992). ''Plasticity models for the biaxial behavior of concrete at elevated temperatures.'' *Computational Methods of Appl. Mech. and Engrg.*, 100, 207–223.

Kontani, O. (1994). ''Experimental determination and theoretical prediction of pore pressure in sealed concrete at sustained high temperatures,'' PhD thesis, Northwestern University, Evanston, Ill.

Laube, M. (1990). ''Constitutive model for the analysis of temperature-stresses in massive structures,'' PhD thesis, TU Braunschweig, Braunschweig, Germany (in German).

Lin, W.-M., Lin, T. D., and Powers-Couche, L. J. (1996). ''Microstructure of fire-damaged concrete.'' *ACI Mat. J.*, 93(3), 199–205.

Mindess, S., Young, J. F., and Lawrence, F.-V. (1978). ''Creep and drying shrinkage of calcium silicate pastes. I: Specimen preparation and mechanical properties.'' *Cement and Concrete Res.*, 8, 591–600.

Noumowé, N. A. (1995). ''Effect of high temperature (20°–600°C) on concrete. The case of high performance concretes,'' PhD thesis, INSA de Lyon, Lyon, France (in French).

Ortiz, M., and Simo, J. C. (1986). ''An analysis of a new class of integration algorithms for elastoplastic constitutive relations.'' *Int. J. Numer. Methods in Engrg.*, 23, 353–366.

Phan, L. T. (1997). ''Fire performance of high-strength concrete: A report of the state-of-the art.'' *Res. Rep. NISTIR 5934*, National Institute of Standards and Technology, Gaithersburg, Md.

Phan, L. T., Carino, N. J., Duthinh, D., and Garboczi, E., eds. (1997). *Proc., Int. Workshop on Fire Performance of High-Strength Concrete, NIST Spec. Publ. 919*, National Institute of Standards and Technology, Gaithersburg, Md.

Powers, G., and Brownyard, T. L. (1948). ''Studies of the physical properties of hardened portland cement paste.'' *Res. Bull. 22*, Portland Cement Association, Skokie, Ill.

Schneider, U. (1982). ''Behavior of concrete at high temperatures.'' *Deutscher Ausschuss fur Stahlbeton*, Heft 337, Verlag Wilhelm Ernst u. Sohn, Berlin.

Simo, J. C., and Hughes, T. J. R. (1997). *Elastoplasticity and viscoplasticity. Computational aspects.* Springer, Berlin.

Torrenti, J.-M. (1992). ''Strength of concrete at very early stages.'' *Bulletin de liaison des laboratoires des ponts et chaussees*, Paris, 179, 31–41 (in French).

Ulm, F.-J., Acker, P., and Lévy, M. (1999). ''The 'Chunnel' fire. II: Analysis of Concrete Damage.'' *J. Engrg. Mech.*, ASCE, 125(3), 283–289.

Ulm, F.-J., and Coussy, O. (1995). ''Modeling of thermochemomechanical couplings of concrete at early ages.'' *J. Engrg. Mech.*, ASCE, 121(7), 785–794.

Ulm, F.-J., and Coussy, O. (1996). ''Strength growth as chemoplastic hardening in early age concrete.'' *J. Engrg. Mech.*, ASCE, 122(12), 1123–1132.

Willam, K. J., and Warnke, E. P. (1975). ''Constitutive model for the triaxial behavior of concrete.'' *IABSE Proc., 19, Seminar on Concrete Structures Subjected to Triaxial Stresses, Paper III-1*, International Association for Bridge and Structural Engineering, Zurich.

APPENDIX IV. NOTATION

The following symbols are used in this paper:

$\mathbf{A}$ = second-order thermomechanical coupling tensor;
A_m = hydration affinity;
$\mathbf{B}$ = second-order chemomechanical coupling tensor;
$\mathbf{C}$ = fourth-order elastic stiffness tensors;
C_ε, $C_{\tau_d/\mathcal{T}\to 0}$ = volume heat capacity and apparent volume heat capacity during dehydration;
D_E = elasticity domain;
$d\lambda$ = plastic multiplier;
E, E_0 = Young's modulus and initial Young's modulus;
E_a = hydration activation energy;
$\mathbf{e}^p$ = plastic strain deviator;
f = loading function;
f_c, f_t, f_{bc} = concrete strength in uniaxial compression, uniaxial tension, and biaxial compression;
G = shear modulus;
H = plastic hardening modulus;
h = plastic hardening coefficient;
$\mathbf{I}$ = fourth-order unit tensor;
K = bulk modulus;
$\mathcal{K}$ = isotropic conductivity coefficient;
k = chemoplastic coupling coefficient;
$\mathcal{L}$ = characteristic length of heat conduction;
l = latent heat of hydration;
$\mathbf{m}_{sk}$, m_0 = hydration mass per volume unit and initial hydration mass per volume unit;
$\mathbf{P}$, $\mathbf{Q}$ = partial derivatives of Willam-Warnke criterion;

$\mathbf{q}$ = heat flux vector;
R = universal constant for ideal gas;
S = entropy;
$\mathbf{s}$ = stress deviator;
T, T_0 = (absolute) temperature and reference temperature (= 293 K);
$\mathcal{T}$ = characteristic time of structural heat conduction;
U = frozen energy;
$\mathbf{u}_i$ = eigenvector associated with principal stress σ_i;
$\mathbf{X}$ = dimensionless position vector;
$\mathbf{x}$ = position vector;
$\dot{x}$ = time derivative of quantity x;
z = isotropic plastic hardening/softening function of concrete;
$\boldsymbol{\alpha}$, α = second-order tensor of thermal dilatation coefficients and isotropic thermal dilatation coefficient;
$\boldsymbol{\beta}$ = second-order chemomechanical coupling tensor;
$\delta(\theta)$, δ_t, δ_c = Willam-Warnke friction angle function and friction angle on tensile and compression meridian;
ε, ε^p = volume strain and plastic volume strain;
$\boldsymbol{\varepsilon}$, $\boldsymbol{\varepsilon}^p$ = strain tensor and plastic strain tensor;
ζ = chemoplastic hardening force;
η = viscous coefficient;
θ = Lode angle;
κ = (de-)hydration equilibrium constant;
$\boldsymbol{\Lambda}$ = elastic compliance tensor;
ν = Poisson's ratio;
ξ, $\xi(T)$ = hydration degree and thermal dehydration function;
ρ, ρ_0 = cohesion pressure and initial cohesion pressure;
σ = mean stress;
$\boldsymbol{\sigma}$ = stress tensor;
σ_i = eigenvalue i of stress tensor;
τ = second stress deviator invariant;
τ_d = characteristic time of dehydration;
φ = dissipation;
φ_1 = plastic dissipation;
φ_c = hydration dissipation;
χ = hardening/softening variable;
Ψ = free energy;
ψ = (elastic) strain energy; and
$\mathbf{1}$ = second-order unit tensor.